

---

*Research Article: New Research | Sensory and Motor Systems*

## **Neuronal activity distributed in multiple cortical areas during voluntary control of the native arm or a brain-computer interface**

<https://doi.org/10.1523/ENEURO.0376-20.2020>

**Cite as:** eNeuro 2020; 10.1523/ENEURO.0376-20.2020

Received: 30 August 2020

Revised: 27 September 2020

Accepted: 1 October 2020

---

*This Early Release article has been peer-reviewed and accepted, but has not been through the composition and copyediting processes. The final version may differ slightly in style or formatting and will contain links to any extended data.*

**Alerts:** Sign up at [www.eneuro.org/alerts](http://www.eneuro.org/alerts) to receive customized email alerts when the fully formatted version of this article is published.

Copyright © 2020 Liu and Schieber

This is an open-access article distributed under the terms of the Creative Commons Attribution 4.0 International license, which permits unrestricted use, distribution and reproduction in any medium provided that the original work is properly attributed.

1 **Title:** Neuronal activity distributed in multiple cortical areas during voluntary control of the native arm or  
2 a brain-computer interface

3 **Abbreviated Title:** Distributed activity during manual or BCI control

4  
5 **Authors:** Zheng Liu<sup>1</sup> and Marc H. Schieber<sup>1,2\*</sup>

6  
7 **Affiliations:**

8 <sup>1</sup>Department of Biomedical Engineering, University of Rochester, Rochester, NY, 14627

9 <sup>2</sup>Department of Neurology, University of Rochester, Rochester, NY, 14642

10

11 **Author Contributions:** Z.L. and M.H.S. designed the study. Z.L. collected the data, performed the  
12 analyses, and wrote the manuscript. M.H.S. supervised, provided resources, and edited the manuscript.

13

14 **\*Corresponding Author:** Please address correspondence to:

15 Marc H. Schieber  
16 Department of Neurology  
17 University of Rochester Medical Center  
18 601 Elmwood Avenue, Box 673  
19 Rochester, NY 14642  
20 E-mail: [mschiebe@ur.rochester.edu](mailto:mschiebe@ur.rochester.edu)

21

22 **Number of Figures:** 10  
23 **Number of Tables:** 3  
24 **Number of Multimedia:** 0  
25 **Number of Words in the Abstract:** 248  
26 **Number of Words in the Significance Statement:** 120  
27 **Number of Words in the Introduction:** 746  
28 **Number of Words in the Discussion:** 2007

29

30 **Acknowledgements:** The authors thank Gil Rivlis for custom task-control software and Marsha Hayles  
31 for editorial comments.

32 **Conflict of Interest Statement:** The authors declare no competing financial interests.

33 **Funding Sources:** This work was supported by grant R01NS092626 to MHS from the National Institute  
34 of Neurological Disorders and Stroke. The funders had no role in study design, data collection or  
35 interpretation, nor in the decision to submit the work for publication.

36 **ABSTRACT**

37 Voluntary control of visually-guided upper extremity movements involves neuronal activity in multiple  
38 areas of the cerebral cortex. Studies of brain-computer interfaces (BCIs) that use spike recordings for input,  
39 however, have focused largely on activity in the region from which those neurons that directly control the  
40 BCI, which we call BCI units, are recorded. We hypothesized that, just as voluntary control of the arm and  
41 hand involves activity in multiple cortical areas, so does voluntary control of a BCI. In two subjects  
42 (*Macaca mulatta*) performing a center-out task both with a hand-held joystick and with a BCI directly  
43 controlled by 4 primary motor cortex (M1) BCI units, we recorded the activity of other, non-BCI units in  
44 M1, dorsal and ventral premotor cortex, primary somatosensory cortex, dorsal posterior parietal cortex, and  
45 the anterior intraparietal area. In most of these areas, non-BCI units were active in similar percentages and  
46 at similar modulation depths during both joystick and BCI trials. Both BCI and non-BCI units showed  
47 changes in preferred direction. Additionally, the prevalence of effective connectivity between BCI and non-  
48 BCI units was similar during both tasks. The subject with better BCI performance showed increased  
49 percentages of modulated non-BCI units with increased modulation depth and increased effective  
50 connectivity during BCI as compared to joystick trials; such increases were not found in the subject with  
51 poorer BCI performance. During voluntary, closed-loop control, non-BCI units in a given cortical area may  
52 function similarly whether the effector is the native upper extremity or a BCI-controlled device.

53

54 **SIGNIFICANCE STATEMENT**

55 Reaching to and grasping a visible object involves neuronal activity in multiple areas of the cerebral  
56 cortex. Whether neurons in these areas are engaged similarly when a subject controls a brain-computer  
57 interface remains unknown. We found similar unit activity in multiple cortical areas as subjects  
58 performed a center-out task with either a hand-held joystick or a brain-computer interface controlled by  
59 only 4 BCI units in the primary motor cortex. Like the 4 BCI units, non-BCI units in most cortical areas  
60 showed changes in their preferred direction between joystick and BCI trials, with similar modulation  
61 depths and effective connectivity. We suggest that a given cortical area may function similarly during  
62 voluntary closed-loop control of either the upper extremity or a BCI.

63 **INTRODUCTION**

64 Voluntary control of movement involves many parts of the central and peripheral nervous system. In the  
65 mammalian cerebral cortex, active regions include the primary motor cortex (M1), dorsal premotor cortex  
66 (PMd), ventral premotor cortex (PMv), primary somatosensory cortex (S1), dorsal posterior parietal cortex  
67 (dPPC), and anterior intraparietal area (AIP) (Rizzolatti et al., 1998; Grafton, 2010). While neural activity  
68 in M1 is primarily responsible for movement execution, concurrent activity in these additional frontal and  
69 parietal areas may be involved in receiving information on goal/target selection for movement planning, in  
70 computing feedforward models of the expected movement, and in processing feedback from the ongoing  
71 movement (Shadmehr and Krakauer, 2008).

72 Brain-computer interfaces (BCIs) now are being developed not only to control prosthetic arms (Hochberg  
73 et al., 2012; Wodlinger et al., 2015; Lebedev and Nicolelis, 2017; Andersen et al., 2019), but also to  
74 investigate nervous system function (Jarosiewicz et al., 2008; Law et al., 2014; Sadtler et al., 2014; Moxon  
75 and Foffani, 2015; Golub et al., 2018; Oby et al., 2019; Zhou et al., 2019). The majority of BCI studies to  
76 date that employ neuron recordings have focused on analyzing the activity of those neurons that contribute  
77 directly to the decoded BCI output, which we refer to as “BCI units.” These BCI units comprise only a  
78 small fraction of the neuronal population active locally, however. Other simultaneously recorded neurons,  
79 which we refer to as “non-BCI units”, have been found to be active along with BCI units, sometimes  
80 changing their patterns of activity in ways similar to the BCI units (Hwang et al., 2013; Arduin et al., 2014;  
81 Law et al., 2014). With few exceptions (Koralek et al., 2012; Bridges et al., 2020), however, these non-BCI  
82 units have been in the same cortical area as the BCI units.

83 Yet just as voluntary control of natural upper extremity movement requires the participation of cortical  
84 areas beyond M1, controlling a closed-loop BCI is likely to require the activity of neurons beyond the BCI  
85 units. The BCI units at least must receive processed visual information on the location of the goal/target,  
86 and probably are affected by processed visual feedback on the motion of the effector as well. Decisions  
87 about when to initiate the next trial, when to start the motion of the effector, and when to stop, all must  
88 reach the BCI units. The firing of the BCI units may also be processed as efference copy, being compared  
89 to an internal model of the expected feedback. Indeed, as human subjects learned to modulate high-gamma  
90 ECoG potentials at one electrode in the motor or premotor cortex, strong parallel activation in prefrontal,  
91 premotor, and posterior parietal cortex appeared and then diminished as learning progressed (Wander et al.,  
92 2013). Whether features of unit activity such as preferred direction and modulation depth change in non-  
93 BCI units distributed across multiple cortical areas remains unknown.

94 We hypothesized that controlling a BCI would entail activity not only of the BCI units, but also of non-BCI  
95 units distributed throughout the multiple cortical areas that participate in natural control of upper extremity  
96 movement. Furthermore, if controlling a BCI required changes in the natural activity patterns of the BCI  
97 units, then the activity patterns of non-BCI units—in terms of preferred direction, modulation depth, and  
98 effective connectivity—potentially could change as well. We therefore trained monkeys already  
99 experienced in a joystick-controlled center-out task to perform a similar task with a novel BCI. Rather than  
100 using a BCI decoder optimized to incorporate the natural tuning of large numbers of M1 neurons (Athalye  
101 et al., 2017; Zhou et al., 2019), we chose a BCI decoder that used only 4 M1 neurons, each assigned  
102 arbitrarily to drive velocity in the one of the 4 cardinal directions. We considered it likely that this decoder,

103 while difficult to learn, would require novel patterns of co-activation among the BCI units and out-of-  
104 manifold reorganization involving non-BCI units as well (Fetz, 1969; Moritz et al., 2008; Nazarpour et al.,  
105 2012; Law et al., 2014; Oby et al., 2019). Moreover, rather than pursuing extensive BCI training to achieve  
106 performance equivalent to that with the hand-held joystick, we chose instead to train a more permissive  
107 task less extensively but repeatedly with different sets of BCI units, enabling us to distinguish consistent  
108 versus inconsistent features in the activity of non-BCI units. After the monkeys acquired a preselected level  
109 of proficiency with each set of BCI units, we compared the activity of non-BCI units in M1, PMd, PMv,  
110 S1, dPPC, and AIP during joystick- versus BCI-control.

111 **METHODS**

112 *Subjects*

113 Two male rhesus monkeys, Q and P (weighing 9-11 kg), were subjects in the present study. All procedures  
114 for the care and use of these nonhuman primates followed the National Institutes of Health Guide for the  
115 Care and Use of Laboratory Animals and were approved by the University Committee on Animal Resources  
116 at the University of Rochester, Rochester, New York.

117 *Center-out task*

118 Each monkey initially was trained to perform a two-dimensional center-out task using a joystick held with  
119 the right hand to control the position of a cursor. The base of the joystick was inclined 30 degrees toward  
120 the primate chair in which the monkey was seated. When centered, the joystick knob was positioned 20 cm  
121 in front of and 5 cm below the monkey's right shoulder. The monkey then could reach all positions within  
122 a 20 cm × 20 cm hand workspace. An LCD screen positioned 90 cm in front of the monkey at eye level  
123 displayed both the cursor and the targets in a square visual workspace divided into 1,000 "screen units"  
124 horizontally and 1,000 screen units vertically.

125 Trials began when the circular center target turned green (Figure 1A). The monkey then positioned the  
126 cursor (white "+") within the center target (Figure 1B) and kept the cursor there for a 500 ms center hold  
127 epoch (Figure 1C). Rather than traditional circular peripheral targets, we used 8 segments of an annulus,  
128 eliminating the possibility that the cursor could pass between targets. When the center hold epoch ended,  
129 the center target turned gray and one of the 8 peripheral targets turned green (Figure 1D), providing a Go  
130 cue that instructed the monkey to move the cursor out of the center target within 2000 ms and into the  
131 instructed peripheral target within another 2000 ms, without entering any other peripheral target (Figure  
132 1E). The center target and the other 7 peripheral targets then disappeared, and monkey was required to keep  
133 the cursor in the peripheral target for a final hold epoch lasting 600 ms (Figure 1F). The end of the final  
134 hold period was designated a Success event. Successful trials were rewarded with a drop of water. If any  
135 of these conditions was not met, however, the trial was aborted immediately, the entire display turned red,  
136 and a 1,500 ms error timeout followed. Every trial was followed by a 1,500 ms inter-trial interval, after  
137 which the center target re-appeared and the subject then could initiate the next trial. Trials were presented  
138 in blocks including 1 each of the 8 peripheral targets presented in a random order that was re-randomized  
139 between blocks. To prevent the monkey from rejecting trials involving particular targets, error trials were  
140 repeated until performed successfully. The entire behavioral task was controlled by custom software  
141 running on a PC which also sent behavioral event marker codes into the collected data stream.

142 *Microelectrode Arrays*

143 Once each monkey was trained to perform the center-out task, Floating Microelectrode Arrays (FMAs;  
144 MicroProbes for Life Sciences) were implanted in six cortical areas using procedures described in detail  
145 previously (Mollazadeh et al., 2011; Rouse and Schieber, 2016). Figure 2 shows the location of the arrays  
146 implanted in M1, PMd, PMv, S1, dPPC, and AIP. Note that our dPPC arrays recorded from the medial  
147 intraparietal area (MIP) in the anterior bank of the intraparietal sulcus as well as adjacent parts of area PE  
148 on the surface of the postcentral gyrus (Bakola et al., 2017; Rajalingham and Musallam, 2017; De Vitis et

149 al., 2019). Except for AIP, all these areas are known to be active during center-out movements  
150 (Georgopoulos et al., 1982; Kalaska et al., 1983; Prud'homme et al., 1994; Batista and Andersen, 2001;  
151 Stark et al., 2007; Rajalingham and Musallam, 2017; De Vitis et al., 2019). For Monkey Q, two 32-channel  
152 FMAs were implanted in each of the six cortical areas, and an additional 16-channel FMA was implanted  
153 in M1. For Monkey P, six 16-channel FMAs were implanted in M1, five in PMd, three in PMv, three in S1,  
154 two in dPPC, and three in AIP; and an additional 32-channel array was implanted in dPPC. The length of  
155 electrodes varied from 1mm to 8mm. All electrodes were made from 70% Pt and 30% Ir and had a nominal  
156 impedance of 0.4 – 0.6 M $\Omega$  at the time of implantation.

### 157 *Neural Data Acquisition*

158 Neural data was collected with two 128-channel Plexon data acquisition systems (Plexon Inc.) and one 128-  
159 channel Cerebus data acquisition system (Blackrock Microsystems). For Monkey Q, all implanted  
160 electrodes could be recorded simultaneously with the three recording systems. For Monkey P, however,  
161 one of the Plexon systems was not available, and the total number of implanted electrodes (384) was greater  
162 than the number of recording channels available (256). Premotor and parietal arrays therefore were grouped  
163 separately and recorded on alternate days along with the M1 arrays (Group 1: M1, PMv, and PMd arrays;  
164 Group 2: M1, S1, AIP, dPPC arrays).

165 Signals from each FMA were amplified by a head stage (gain 20 $\times$  for the Plexon systems, 2 $\times$  for the Cerebus  
166 system) and further amplified by the data acquisition hardware before being digitized and stored to disk by  
167 the host PCs for each system. For the Plexon systems, spike waveforms that crossed a threshold selected  
168 interactively on-line were sampled at 40 kHz using Sort Client (Plexon, Inc.), with additional sorting off-  
169 line. For the Cerebus system, broadband signals were sampled at 30 kHz, and spikes were extracted off-  
170 line and sorted with custom Matlab (Mathworks) scripts. Both single units and multi-units were included  
171 in analyses, whereas any sorted units with a signal-to-noise ratio (SNR) < 2.5 were discarded. Behavioral  
172 event marker codes generated by the task control PC were used to synchronize the data recorded by different  
173 acquisition systems for analysis.

### 174 *BCI control*

175 BCI experiments were performed 6 – 14 months after surgical implantation of microelectrode arrays. Daily  
176 recording sessions started with ~200 joystick-controlled trials, followed by trials in which the monkey's  
177 arm was restrained in the primate chair and the cursor was controlled through a brain-computer interface.  
178 Neural data were recorded continuously throughout both joystick- and then BCI-controlled trials.

179 To control the BCI, four units were chosen randomly from a pool of ~10 – 20 candidate M1 units (either  
180 single units or multi-units) that had been recorded stably on-line for at least 5 days. These four units were  
181 assigned randomly by a Matlab script to drive cursor velocity in the four cardinal directions: rightward,  
182 leftward, upward, or downward. The directional assignment of each of these BCI units was made without  
183 consideration of its preferred direction during joystick trials.

184 The firing rate of each BCI unit controlled the output of a separate linear velocity decoder that moved the  
 185 cursor in the assigned cardinal direction. The output of each velocity decoder at time  $t$ ,  $v(t)$ , was calculated  
 186 as:

$$187 \quad v(t) = \frac{A}{\sqrt{FR^{80\%}} - \sqrt{FR^{20\%}}} \times (\sqrt{FR(t)} - \sqrt{FR^{20\%}}) - \frac{A}{2} \quad (1)$$

188 where  $FR(t)$  is the instantaneous firing rate of the BCI unit estimated using spike counts in 10 ms bins  
 189 convolved with a 500 ms Gaussian filter and  $A$  is an empirical value set to 6 screen units per 10 ms. Square-  
 190 root transformation of the unit's firing rate was used to reduce variance (Kihlberg et al., 1972; Ashe and  
 191 Georgopoulos, 1994; Rouse and Schieber, 2016). The 80<sup>th</sup> percentile and 20<sup>th</sup> percentile of the BCI unit's  
 192 firing rate distribution,  $FR^{80\%}$  and  $FR^{20\%}$ , were estimated initially from the cumulative distribution of  
 193 firing rates recorded during joystick-controlled trials before beginning the BCI task each day. To adjust for  
 194 firing pattern changes between joystick control and BCI control,  $FR^{80\%}$  and  $FR^{20\%}$  were updated after the  
 195 first 5 minutes of BCI control using the cumulative distribution of firing rates during that interval. To  
 196 prevent surges on individual BCI-unit decoders,  $v(t)$  was limited to the range of  $\pm 3$  screen units/10 ms.  
 197 The cursor's horizontal and vertical velocities then were determined independently, each in a "push-pull"  
 198 fashion based on the output of the four velocity decoders driven separately by the four BCI units ( $v_{right}$ ,  
 199  $v_{left}$ ,  $v_{up}$ ,  $v_{down}$ ):

$$200 \quad v_{horizontal} = v_{right} - v_{left} \quad (2)$$

$$201 \quad v_{vertical} = v_{up} - v_{down} \quad (3)$$

202 For example, if  $v_{right} = 2.5$ ,  $v_{left} = -0.3$ ,  $v_{up} = -0.2$ ,  $v_{down} = -2.3$ , then  $v_{horizontal} = 2.8$ ,  $v_{vertical} = 2.1$ , the  
 203 resultant cursor velocity was 3.5 ( $= \sqrt{2.8^2 + 2.1^2}$ ) screen units/10 ms at  $37^\circ$  ( $= \tan^{-1}(2.1/2.8)$ ). Cursor  
 204 position was updated every 10 ms.

### 205 *BCI training*

206 As expected from previous work (Law et al., 2014; Sadtler et al., 2014; Oby et al., 2019), learning to control  
 207 the cursor with four arbitrarily assigned M1 units proved challenging for both monkeys. We therefore  
 208 relaxed the criteria for successful trial completion to a level at which the monkeys persevered in learning  
 209 to control the BCI rather than becoming excessively frustrated. The center hold epoch was reduced to 20  
 210 ms; the final hold epoch was reduced to 50 ms; the subjects were allowed up to 5,000 ms to move the cursor  
 211 out of the center target once the peripheral target had appeared, and 5,000 ms more to move the cursor into  
 212 the correct peripheral target after leaving the center target. In addition, during the movement to the  
 213 peripheral target (Figure 1E), the subjects were allowed to enter peripheral targets other than the instructed  
 214 target. Each monkey then could be trained over several days to control the BCI using the four M1 units  
 215 each acting in their arbitrarily assigned direction. If a BCI unit driving cursor motion in a given direction  
 216 was lost to isolation during this period, we assigned another M1 unit to that direction using the same criteria  
 217 described above.

218 Figure 3 illustrates the progress of BCI training in sequential blocks of 50 correctly performed trials.  
219 Training began with a one-dimensional BCI task, initially presenting only the upward and downward targets  
220 (Figure 3, 1D vertical) and then only the rightward and leftward targets (Figure 3, 1D horizontal). One-  
221 dimensional training continued for 5 days (block 33) until the monkey performed successfully in ~ 80% of  
222 the trials for each dimension separately. Thereafter, the monkey was trained to control two-dimensional  
223 cursor movement to all eight peripheral targets, reaching a plateau of relatively stable performance with  
224 success rates > 80% after another few days (block 58). As the success rate rose, the response time—from  
225 the Go cue until the end of the final hold epoch—fell.

226 We refer to the set of four M1 units selected to simultaneously control the BCI as a BCI-unit “assignment.”  
227 Once a subject had reached a stable plateau at success rates > 80% and data had been collected with one  
228 such assignment, a new BCI-unit assignment was selected randomly using the criteria described above,  
229 with the additional restriction that a given M1 unit was not assigned to control the same direction in more  
230 than one assignment. The BCI training process then was repeated, starting with one-dimensional BCI  
231 training and progressing to two-dimensional training, and additional data was collected after the monkey’s  
232 performance again had reached a plateau at success rates > 80%. Monkey Q was trained to this level with  
233 five different BCI-unit assignments, and monkey P with three. Initial one-dimensional training required an  
234 average of  $5.6 \pm 3.1$  days (mean  $\pm$  SD across BCI-unit assignments) for Monkey Q and  $5.7 \pm 0.6$  days for  
235 monkey P. Two-dimensional training then required another  $6.4 \pm 1.1$  days for Monkey Q and  $9.0 \pm 3.6$   
236 days for Monkey P.

### 237 *Experimental Design and Statistical Analyses*

238 For each BCI-unit assignment, we analyzed neural data collected once the subjects were performing the  
239 two-dimensional BCI task at a success rate > 80%. We selected for analysis sessions in which the subject  
240 had performed at least 400 BCI trials successfully. These sessions also included ~ 200 successfully  
241 performed joystick-controlled trials. To compare equal numbers of trials during BCI versus joystick  
242 control, in each analyzed session we identified the maximum number of successful trials to each target  
243 common to both BCI control and joystick control. For Monkey P, comparing across cortical areas also  
244 required analyzing two different sessions, one in which premotor areas had been recorded and another in  
245 which parietal areas had been recorded, and we therefore found the maximum number of successful trials  
246 common to both tasks in both sessions. We then randomly selected that number of trials for analysis from  
247 each type of task in each session, which typically selected all the joystick trials but only ~ 30% to 50% of  
248 the BCI trials.

249 Chronically implanted microelectrode arrays often record some of the same units repeatedly in daily  
250 sessions over months. To prevent the same unit from being included repeatedly in our analyses, we  
251 identified unit recordings that probably originated from the same neuron recorded on different days. The  
252 similarity of units recorded from the same electrode was evaluated using four metrics: pairwise cross-  
253 correlograms, autocorrelograms, waveform shape, and mean firing rate (Fraser and Schwartz, 2012;  
254 Downey et al., 2018). A decision boundary of whether two unit recordings came from the same neuron was  
255 drawn using a quadratic classifier under the assumption that the data could be modeled as a mixture of  
256 multivariate Gaussians. When two or more units were labeled as having been recorded from the same  
257 neuron across days, we retained for the present analyses only the unit with the highest SNR and excluded

258 the others. In this manner 103 of 531 units recorded from Monkey Q and 212 of 823 units from Monkey P  
 259 were excluded from the following analyses. The left number in each cell of Table 1 gives the number of  
 260 unique units remaining for analysis in each cortical area for each of the five assignments from monkey Q  
 261 and three from monkey P.

#### 262 Task-related modulation

263 Neuron firing rates in several cortical areas often show cosine tuning as subjects perform a center-out task  
 264 (Georgopoulos et al., 1982; Kalaska et al., 1983; Prud'homme et al., 1994; Moran and Schwartz, 1999). We  
 265 therefore considered a unit to be modulated in relation to the center-out task if its firing rate was fit by a  
 266 classical cosine tuning function:

$$267 \quad f(\theta) = \alpha + \beta \times \cos(\theta - \theta_{PD}) \quad (4)$$

268 at a significance level of  $p < 0.05$  ( $F$ -test; Matlab “regress” function). In equation 4,  $f(\theta)$  is the firing rate  
 269 when the peripheral target was centered at  $\theta^\circ$  (the eight peripheral targets in Figure 1D were assigned to  
 270  $0^\circ$  to  $315^\circ$  at  $45^\circ$  intervals);  $\alpha$  is the baseline firing rate,  $\beta$  is the absolute modulation depth, and  $\theta_{PD}$  is the  
 271 preferred direction (PD) of the unit. Each unit was tested for a cosine fit separately using joystick trials and  
 272 using BCI trials. The center and right numbers of each cell in Table 1 give the numbers of units significantly  
 273 cosine-tuned in joystick and/or BCI trials, and in both joystick and BCI trials, respectively.

#### 274 Preferred direction change ( $\Delta PD$ )

275 We estimated the preferred direction change ( $\Delta PD$ ) between joystick trials and BCI trials for each unit that  
 276 was cosine tuned in both tasks by calculating the difference between the unit’s preferred direction during  
 277 joystick trials ( $\theta_{PD\_Joystick}$ ) and BCI trials ( $\theta_{PD\_BCI}$ ):

$$278 \quad \Delta PD = \theta_{PD\_BCI} - \theta_{PD\_Joystick} \quad (5)$$

279 To determine the statistical significance of each unit’s  $\Delta PD$ , we employed a bootstrap procedure (Chestek  
 280 et al., 2007). For each unit, we calculated a distribution of PDs by randomly sampling with replacement  
 281 1,000 times for joystick trials and for BCI trials separately. For each of these two distributions, the mean  
 282 was subtracted, producing a zero-mean distribution of PDs for joystick trials and for BCI trials. Then a  
 283 distribution of  $BCI - Joystick$   $\Delta PD$ s was gathered by randomly selecting one PD from the zero-mean BCI  
 284 trial distribution and one from the zero-mean Joystick distribution, calculating the difference, and repeating  
 285 1,000 times, providing a bootstrap  $\Delta PD$  distribution for that unit under the null hypothesis of no BCI –  
 286 Joystick difference (i.e. both with mean = 0). The actual  $\Delta PD$  for that unit then was compared with this  
 287 bootstrap  $\Delta PD$  distribution. If the actual  $\Delta PD$  was higher than the 97.5<sup>th</sup> percentile or lower than the 2.5<sup>th</sup>  
 288 percentile of the bootstrap  $\Delta PD$  distribution, we considered the unit to have had a significant  $\Delta PD$ . This  
 289 process was repeated for each unit separately.

290 We also examined  $\Delta PD$ s at the population level to determine whether the entire population rotated to some  
 291 degree coherently in the same direction resulting in a net change, or whether different units changed in  
 292 random directions with no net change in the population. If the median of actual  $\Delta PD$ s was significantly

293 different from  $0^\circ$  (circular rank-sum test, `circ_medtest` function, Matlab CircStat toolbox (Berens, 2009)),  
 294 we considered that the population had a significant degree of coherent rotation.

#### 295 Normalized modulation depth

296 To compare the modulation of units with different baseline firing rates, we calculated a normalized  
 297 modulation depth ( $nMD$ ) for each unit that was significantly cosine-tuned during each task separately  
 298 (joystick or BCI) using the unit's absolute modulation depth during that task ( $\beta$ , equation 4):

$$299 \quad nMD = \frac{\beta \times 2}{FR^{80\%} - FR^{20\%}} \quad (6)$$

300 Unlike the values used for BCI units on-line (equation 1), here  $FR^{80\%}$  and  $FR^{20\%}$  are the 80<sup>th</sup> percentile  
 301 and 20<sup>th</sup> percentile, respectively, of the overall firing rate distribution pooling data from both joystick and  
 302 BCI trials. This  $nMD$  for either joystick trials or BCI trials therefore could be  $> 1$  if the unit was modulated  
 303 intensely in one of the tasks and had relatively low firing rates during the other. In general, the higher the  
 304  $nMD$ , the more intensely the unit was modulated.

#### 305 Effective connectivity analysis

306 To examine effective connectivity among simultaneously recorded units, we used Granger causality  
 307 adapted for point processes (Kim et al., 2011; Balasubramanian et al., 2017). This adaptation replaces the  
 308 standard multivariate vector autoregressive models with point process likelihood functions, where the point  
 309 process of a spike train is characterized by the logarithm of a conditional intensity function (CIF) modeled  
 310 with a generalized linear model (GLM). To optimize both the temporal resolution of the models and the  
 311 ability to detect effective connectivity at various latencies, CIFs were calculated with durations from 3 ms  
 312 to 99 ms in 3 ms steps, and the resulting GLM that provided the best approximation of the spike trains was  
 313 selected using Akaike's information criterion (AIC). The optimal spike histories determined in this way  
 314 had a median duration of 12 ms and 90<sup>th</sup> percentile of 51 ms.

315 For each unit,  $i$ , the point process likelihood then was modeled first with covariates including the spiking  
 316 history of that unit and all other simultaneously recorded units, characterized by a parameter vector,  $\gamma_i$ ,  
 317 and second with the same covariates but excluding the spiking history of another unit,  $j$ , characterized by  
 318 parameter vector denoted,  $\gamma_i^j$ . The log-likelihood ratio for these two models then is,  $\Gamma_{ij}$ :

$$319 \quad \Gamma_{ij} = \log \frac{L_i(\gamma_i^j)}{L_i(\gamma_i)} \quad (7)$$

320 Because excluding the information provided by unit  $j$  can only degrade the modeling of unit  $i$  and decrease  
 321 the likelihood  $L_i(\gamma_i^j)$  relative to  $L_i(\gamma_i)$ , the ratio of likelihoods is always  $\leq 1$  and the log likelihood ratio is  
 322 always  $\leq 0$ , theoretically being  $= 0$  if unit  $j$  has no effect on unit  $i$  and increasingly  $< 0$  the stronger the  
 323 effect. A Granger Causality Measure (GCM),  $\Phi_{ij}$ , then can be calculated as:

$$324 \quad \Phi_{ij} = -\text{sign}(\gamma_i^j) \Gamma_{ij} \quad (8)$$

325 where positive values indicate an excitatory effect of unit  $j$  on unit  $i$  and negative values indicate an  
 326 inhibitory effect.

327 This analysis was performed using all  $Q$  simultaneously recorded spike trains from 750 ms before to 2250  
 328 ms after the Go cue in each analyzed trial, providing a  $Q \times Q$  matrix of GCMs, the  $\Phi_{ij}$ , i.e. the strength of  
 329 the effect of  $j^{\text{th}}$  unit on the  $i^{\text{th}}$  unit. Significance testing was performed on the  $\Gamma_{ij}$ , the distribution of which  
 330 approaches the  $X^2$  distribution for large  $Q$ . The Benjamini–Hochberg procedure was applied to control the  
 331 false discovery rate at 0.05. The Granger connectivity of each unit  $j$  to unit  $i$  then was classified as i) no  
 332 significant connectivity, ii) significant excitatory connectivity, or iii) significant inhibitory connectivity.

333 We performed a simulation to examine the extent that identifying effective connectivity in this way would  
 334 be influenced by the modulation depth of the unit pair being tested. We simulated a population of 30 units:  
 335 15 units with a relatively low  $nMD$  of 0.35, and 15 with a relatively high  $nMD$  of 0.75. For each unit, we  
 336 generated spike trains in 1 ms bins for 10 trials to each of the 8 targets, all lasting 1 second. Each unit was  
 337 assigned a randomly generated preferred direction with a baseline firing rate,  $FR_{baseline}$ , drawn from a  
 338 uniform distribution in the range [10, 30] Hz. The average  $FR_{baseline}$  thus was 20 Hz for both low  $nMD$  and  
 339 high  $nMD$  populations. Spikes of unit  $i$  for a simulated trial with a target located at  $\theta^\circ$  were generated using  
 340 a commonly used procedure (Koch, 2004; Kim et al., 2011). At each 1ms time step, a random number  
 341 uniformly distributed in the range [0, 1] was generated and compared to a threshold,  $\delta_\theta^i$ , based on cosine  
 342 directional tuning with the unit's baseline firing rate ( $FR_{baseline}^i$ ), modulation depth ( $MD^i$ ), and preferred  
 343 direction ( $\theta_{PD}^i$ ):

$$344 \quad \delta_\theta^i = \frac{1000}{FR_{baseline}^i + MD^i \times \cos(\theta - \theta_{PD}^i)} \quad (9)$$

345 If the randomly generated number was smaller than  $\delta_\theta^i$ , a spike was simulated to occur in that 1ms bin  
 346 unless a spike had occurred in the one preceding bin (1ms refractory period).

347 Within this population of 30 neurons, we created 12 artificial connections: 3 excitatory connections and 3  
 348 inhibitory connections from a low  $nMD$  unit to another low  $nMD$  unit, and 3 excitatory connections and 3  
 349 inhibitory connections from a high  $nMD$  unit to another high  $nMD$  unit. The target unit of each excitatory  
 350 (or inhibitory) connection was assigned a 50% higher (or lower) likelihood of firing a spike at time  $t$  if the  
 351 trigger unit had fired a spike at any time in the range from  $t-10$  to  $t-6$  ms. We then ran 1,000 simulations  
 352 using the methods described above (equations 7 and 8), for each simulation seeding the population with re-  
 353 randomized  $FR_{baseline}^i$  and  $\theta_{PD}^i$ . All 12 artificial connections were detected in every simulation. Of the  
 354 858 potential false positive connections tested for which no artificial connection was present ( $858 = 30^2$   
 355 potential connections – 30 self connections – 12 true positives), no more than 13 false positives were  
 356 detected ( $13/858 = 0.015$ ) in any of one the 1,000 simulations, with an average false positive rate of 0.0021  
 357 across the 1,000 simulations, all within our accepted false discovery rate of 0.05. Furthermore, the false  
 358 positive rate among the low-low  $nMD$  pairs averaged across simulations was 0.0020; among low-high pairs,  
 359 0.0019; among high-low pairs, 0.0021; and among high-high pairs 0.0025. These false positive rates were  
 360 significantly different among the four connection groups ( $p < 0.005$ , Kruskal-Wallis tests), due to a higher  
 361 false positive rate among high-high pairs compared to low-low pairs ( $p < 0.005$ , post-hoc Kruskal-Wallis  
 362 tests with Bonferroni correction). Although the difference of  $\sim 0.0005$  (5 false positives in 10,000 tests)

363 between low-low pairs and high-high pairs might have contributed an extra high-high false positive  
364 connection to the populations tested (~1,000 tests per population) in the Results below, such a small  
365 difference would not have altered any of the findings described.

366

367 **RESULTS**368 *Behavioral performance during joystick and BCI trials*

369 In each session, the monkey performed the center-out task first using the joystick and then the BCI, both  
370 within ~ 2 hours. Monkey Q was trained to proficient BCI performance—sessions with  $\geq 400$  successfully  
371 performed BCI trials at a success rate  $\geq 80\%$ —with five different BCI-unit assignments, monkey P with  
372 three. For each assignment, we selected for the present analyses a session recorded once the monkey had  
373 been performing at this level consistently. For Monkey Q the selected sessions were recorded 16, 9, 10, 7,  
374 and 10 days after training with a new BCI-unit assignment began; for Monkey P, in which two sessions  
375 were required to record from all cortical areas, after 16/17, 10/11 and 13/14 days. Across these analyzed  
376 sessions, monkey Q performed at a higher success rate during BCI trials than during joystick trials (BCI,  
377  $94.7 \pm 1.4\%$ ; joystick,  $76.6 \pm 3.6\%$ ;  $p < 1e-16$ ,  $\chi^2$  test) whereas Monkey P's success rates were similar  
378 (BCI,  $85.7 \pm 5\%$ ; joystick,  $86.5 \pm 5.7\%$ ;  $p = 0.32$ ,  $\chi^2$  test). Although Monkey P performed at a higher  
379 success rate than Monkey Q during joystick trials ( $p < 5e-12$ ,  $\chi^2$  test), Monkey Q performed at a higher  
380 success rate than Monkey P during BCI trials ( $p < 1e-16$ ).

381 Though both monkeys met our criteria for proficient BCI control during these analyzed sessions, their  
382 performance in BCI trials was not equivalent to that in joystick trials. As detailed in the Methods, because  
383 our arbitrary assignment of BCI units to the four cardinal directions made learning to use each decoder  
384 quite challenging, we relaxed the criteria for successful performance of BCI trials as compared to joystick  
385 trials. Figure 4 compares the cursor trajectories of 5 successful joystick trials and 5 successful BCI trials  
386 (thin lines) involving each of the 8 targets, as well as the average over 20 trials each (thick lines), all from  
387 the same session. Whereas the cursor moved in relatively straight paths in individual joystick trials, in  
388 individual BCI trials the trajectories often were convoluted, though on average directed to the target.

389 We quantified these differences by measuring the path length and the response time, both from the time of  
390 the Go cue to the Success, in all analyzed trials. Pooling across the analyzed sessions from each monkey,  
391 path lengths were longer during BCI trials in both monkeys (Monkey Q, joystick,  $486 \pm 104$  screen units  
392 [mean  $\pm$  standard deviation], BCI,  $755 \pm 348$  screen units,  $p < 5e-44$ , Wilcoxon rank sum test; Monkey P,  
393 joystick,  $507 \pm 110$  screen units, BCI,  $863 \pm 423$  screen units,  $p < 5e-47$ ). Response times also were longer  
394 in BCI trials for Monkey P (joystick,  $1.31 \pm 0.20$  sec; BCI,  $2.20 \pm 1.19$  sec;  $p < 5e-29$ , Wilcoxon rank sum  
395 test), though not for Monkey Q (joystick,  $1.44 \pm 0.33$  sec; BCI,  $1.66 \pm 0.84$  sec,  $p = 0.16$ ). These  
396 performance measures also showed additional differences between monkeys. During joystick trials  
397 Monkey P had shorter paths and response times than Monkey Q (path lengths:  $p < 5e-3$ , response times:  
398  $p < 1e-9$ , Wilcoxon rank sum tests), while during BCI trials Monkey Q had shorter paths and response times  
399 than Monkey P (path lengths:  $p < 5e-4$ , response times:  $p < 5e-11$ ). Although Monkey P's joystick  
400 performance was superior in every measure to that of Monkey Q, Monkey Q's BCI performance was  
401 superior to that of Monkey P.

402 *Neurons in multiple cortical areas were modulated during both joystick and BCI trials*

403 We tested each analyzed unit for cosine tuning separately during joystick trials and during BCI trials, using  
404 the unit's firing rate averaged from the Go cue to Success in each analyzed trial. The leftmost pair of bars

405 in Figure 5 shows the percent of BCI units and the other pairs of bars the percent of non-BCI units in each  
406 cortical area that were cosine tuned during the joystick task (white) and during the BCI task (grey) averaged  
407 across all BCI-unit assignments in each monkey. Colored circles with connecting lines show the  
408 percentages in each assignment separately. With a few exceptions, 25% (arbitrarily chosen level, dashed  
409 horizontal line) or more of the sorted units in each cortical area were modulated during both tasks in each  
410 assignment. Task-related modulation of non-BCI units thus was common in all six cortical areas not only  
411 during joystick control of the cursor, but also during BCI control.

412 On average, 75 to 80% of the BCI units in each monkey were modulated significantly during joystick trials  
413 (Figure 5, BCI units, white bar), whereas during BCI trials 100% of the BCI-units were modulated  
414 significantly for every BCI assignment in both monkeys (Figure 5, BCI units, grey bar). Did the percentage  
415 of modulated non-BCI units also increase during BCI control? In monkey Q, this percentage tended to  
416 increase during BCI control as compared to joystick control. This increase was significant when non-BCI  
417 units were pooled across sessions and across all 6 cortical areas (McNemar's test,  $p < 1e-7$ ). Post-hoc  
418 pairwise testing for individual cortical areas showed significant increases among non-BCI units in M1,  
419 PMd, and AIP (McNemar's test with Bonferroni correction,  $p < 0.0083 = 0.05/6$  cortical areas). Monkey P,  
420 however, did not show any significant changes in the percentage of non-BCI units modulated during BCI-  
421 versus joystick-control. Monkey Q but not Monkey P thus had more modulated non-BCI units in some  
422 cortical areas during BCI control than during joystick control. In monkey Q, this increase in modulated  
423 units may have contributed to superior performance during BCI trials as compared to monkey P.

#### 424 *Non-BCI units in multiple cortical areas changed preferred direction during BCI trials*

425 Given that the firing rate of most of BCI units and many non-BCI units modulated with both joystick and  
426 BCI trials, we compared the preferred direction (PD) of individual units that were significantly cosine-  
427 tuned during both tasks (Table 1, right number in each cell). Figure 6 shows, for example, the change in  
428 preferred direction ( $APD = PD_{BCI} - PD_{Joystick}$ ) for the 4 BCI units (blue) and the 29 non-BCI M1 units (red)  
429 from a single session, along with the bootstrapped distribution of the combined population (BCI and non-  
430 BCI units) expected if there were no changes in PDs.

431 All four BCI units in this illustrated session had a significant preferred direction change between joystick  
432 and BCI trials. Across all assignments, only 1 of the 26 BCI units that were tuned during both tasks did  
433 not show a significant change in the preferred direction between joystick and BCI trials. Did the preferred  
434 directions of BCI units change toward the cardinal directions to which they had been assigned arbitrarily  
435 by the decoder? Knowing the direction assigned to each BCI unit, we calculated the absolute value of the  
436 difference between that assigned direction and the preferred direction of each BCI unit during joystick trials  
437 and again during BCI trials. Across all 26 testable BCI units, this absolute assigned-preferred direction  
438 difference was significantly smaller for BCI than for joystick trials (Monkey Q,  $p < 5e-5$ ; Monkey P,  $p <$   
439  $0.05$ , Wilcoxon rank-sum tests). As might have been expected, therefore, the PDs of BCI units on average  
440 changed toward their assigned directions.

441 Of the 29 non-BCI units illustrated in Figure 4, the preferred directions of 21 (72%) also changed  
442 significantly. And pooling across assignments, the majority of the non-BCI units in each cortical area in

443 each monkey showed significant changes in PD with the exceptions of dPPC and AIP in Monkey Q (Table  
444 2). Changes in PD thus were common among non-BCI units in both monkeys.

445 Systematic changes in PD at the population level can provide insight into the strategy used to perform a  
446 BCI task. In particular, an average  $\Delta PD$  significantly different from  $0^\circ$  suggests a re-aiming strategy in that  
447 most PDs are shifted in the same direction. Re-aiming may provide a useful strategy when the directions  
448 assigned to BCI units on average constitute a relatively consistent rotation of their natural PDs. The 4 BCI  
449 units used here in a given assignment were too few to assess consistent rotation statistically, however. We  
450 therefore classified each BCI unit with a significant  $\Delta PD$  as having a  $\Delta PD < 180^\circ$ ,  $= 180^\circ$ , or  $> 180^\circ$ . Five  
451 of the eight BCI-unit assignments included at least one BCI unit with  $\Delta PD < 180^\circ$  and at least one with  
452  $\Delta PD > 180^\circ$ , making a re-aiming strategy unlikely.

453 For populations of non-BCI units pooled across all cortical areas or within individual cortical areas, a  
454 median  $\Delta PD$  significantly different from  $0^\circ$  was found in only one of the eight assignments (Qiii, circular  
455 rank-sum test,  $p < 0.05/8$  assignments). Significant differences from  $0^\circ$  were not found in any of the  
456 individual cortical areas for any of the BCI-unit assignments. The  $\Delta PD$ s of individual non-BCI units thus  
457 occurred in various directions and amplitudes, resulting in no net  $\Delta PD$  for any population. Considering the  
458 non-BCI units as a surrogate indicator, these findings suggest that, except perhaps in one assignment, the  
459 directions assigned to BCI units did not provide a consistent rotation of their natural preferred directions as  
460 assessed during joystick trials.

461 *Normalized modulation depth increased in some cortical areas during BCI-control*

462 As might have been expected of the BCI units, all of which became modulated during BCI trials, their  
463 average modulation depth also increased during BCI trials as compared to joystick trials in each monkey.  
464 As illustrated in Figure 7 (left), this increase in average  $nMD$  among BCI units occurred consistently in all  
465 sessions in both monkeys. At the level of individual units,  $nMD$  increased in 17 of the 20 BCI units in  
466 Monkey Q and 8 of 12 units in Monkey P during BCI as compared to joystick trials. Similarly, among non-  
467 BCI units  $nMD$  often increased during BCI trials, though less consistently than among BCI units. Figure 7  
468 shows that in each cortical area except dPPC, the median  $nMD$  of non-BCI units increased during BCI trials  
469 in 3 or more of the 5 assignments for Monkey Q, and in 2 or more of the 3 assignments for Monkey P. We  
470 therefore compared  $nMD$  during joystick versus BCI trials for non-BCI units in all six cortical areas. For  
471 this comparison, we included units that showed significant modulation during either joystick or BCI trials,  
472 or both (Table 1, center number in each cell). Pooling across all assignments and cortical areas, the median  
473  $nMD$  of non-BCI units was greater during BCI trials than during joystick trials in monkey Q though the  
474 trend fell short of significance in Monkey P (Monkey Q,  $p < 5e-11$ ; Monkey P,  $p = 0.058$ ; Wilcoxon signed-  
475 rank tests). Post-hoc testing for each cortical area separately (gray vs. white bars in Figure 7) showed  
476 significant increases in M1, PMd, and PMv in Monkey Q (Wilcoxon signed-rank test with Bonferroni  
477 correction,  $p < 0.05/6$ ). As for the increase in the percentage of non-BCI units that were modulated during  
478 BCI trials in monkey Q, this increase in modulation depth may have contributed to superior performance  
479 during BCI trials as compared to monkey P.

480 Modulation depth also varied to some degree among cortical areas. Pooling the data across assignments we  
481 found no significant differences in  $nMD$  among cortical areas during joystick trials in either monkey

482 (Monkey Q,  $p = 0.73$ ; Monkey P,  $p = 0.09$ ; Kruskal-Wallis tests). During BCI trials, however, the variation  
483 in  $nMD$  among cortical areas was significant in each monkey (Monkey Q,  $p < 5e-3$ ; Monkey P,  $p < 1e-3$ ,  
484 Kruskal-Wallis tests). Post-hoc pairwise comparisons revealed that in Monkey Q the median  $nMD$  of non-  
485 BCI units in M1 or in PMv was significantly larger than in dPPC, and in Monkey P the median  $nMD$  of  
486 non-BCI units in M1 or in PMd was larger than in dPPC ( $p < 0.0083 = 0.05/6$ , Kruskal-Wallis tests with  
487 Bonferroni correction for 6 cortical areas). Differences in  $nMD$  between cortical areas thus appeared during  
488 BCI trials that were not present during joystick trials. Modulation in M1 and premotor areas became larger  
489 than that in dPPC, which may have reflected increased modulation in frontal motor areas and/or a decrease  
490 in proprioceptive feedback to dPPC during BCI trials as compared to joystick trials.

#### 491 *Effective connectivity during joystick and BCI trials*

492 The changes observed in the percent of units modulated, their preferred directions, and their normalized  
493 modulation depths suggest that non-BCI units in multiple cortical areas participated indirectly in controlling  
494 the BCI, either influencing the activity of the BCI units, or being influenced by the BCI units, or both. We  
495 therefore compared effective connectivity among both BCI and non-BCI units during joystick trials and  
496 during BCI trials. We evaluated pairwise effective connectivity among all BCI units (Table 1, top row, left  
497 number) and all non-BCI units that were modulated significantly during both joystick and BCI trials (Table  
498 1, other rows, right number in each cell) using Granger causality adapted for point process models (Kim  
499 et al., 2011; Balasubramanian et al., 2017), as described in the Methods. Figure 8 shows the Granger  
500 connectivity matrices from an example session, computed using equal numbers of joystick (A) and BCI (B)  
501 trials. Among the 29 simultaneous recorded units, pairs with excitatory effective connectivity from the  
502 trigger unit (abscissa) to the target unit (ordinate) are indicated by a red square and those with inhibitory  
503 connectivity by a dark blue square.

504 Comparing effective connectivity during joystick versus BCI trials shows that changes occurred both within  
505 and between cortical areas, and both with BCI and with non-BCI units. For the example session shown in  
506 Figure 8, the number of connected pairs increased in many instances—for example: from the BCI units to  
507 non-BCI units in M1, from non-BCI units in M1 to other non-BCI units in M1, and from non-BCI M1 units  
508 to those in PMv—while decreasing in others—for example from PMv units to other PMv units). Overall,  
509 the fraction of significantly connected pairs in this session was greater during BCI than during joystick  
510 trials.

511 Pooling across sessions and across cortical areas in Monkey Q, the fraction of unit pairs with effective  
512 connectivity was significantly larger during BCI trials (Figure 9A, left, grey bar) than during joystick  
513 trials (Figure 9A, left, white bar) in Monkey Q ( $p < 1e-13$ , McNemar's test) but not in Monkey P (Figure  
514 9B, left  $p > 0.6$ ). The increase during BCI trials remained evident in Monkey Q when excitatory ( $p < 5e-8$ )  
515 and inhibitory ( $p < 5e-6$ ) connections were considered separately (Figure 9A, right), but the fraction of  
516 neither excitatory ( $p > 0.1$ ) nor inhibitory ( $p > 0.4$ ) connections changed in Monkey P (Figure 9B, right).  
517 In Monkey Q, this increase in effective connectivity during BCI trials was present in four of the five  
518 individual assignments (Figure 9 A, colored lines). Again, increased effective connectivity may have  
519 contributed to Monkey Q's superior performance during BCI trials as compared to monkey P.

520

521 *Non-BCI units with effective connectivity to or from a BCI unit*

522 Non-BCI units with effective connectivity either to or from a BCI unit might influence BCI control more  
523 strongly than those without such connections. An increase of modulation depth in a non-BCI unit with  
524 effective connectivity to a BCI unit, for example, might have a greater impact on that BCI unit than the  
525 same increase in a non-BCI unit without such connectivity. We therefore divided the non-BCI units into  
526 two groups: Connect+ units had significant excitatory or inhibitory connectivity, either as a trigger or as a  
527 target, with at least one BCI unit; Connect- units had no significant effective connectivity with any of the  
528 BCI units, although Connect- units might or might not have effective connectivity with other non-BCI units.  
529 Table 3 gives the percentages of Connect+ units in each cortical area, pooled across assignments in each  
530 monkey, for both joystick and BCI trials, and further subdivides the Connect+ units into those being the  
531 trigger for versus the target of connectivity with a BCI unit.

532 In both monkeys, pooling across cortical areas revealed an overall increase in the percent of Connect+ units  
533 during BCI trials as compared to joystick trials (Monkey Q, 36% vs 21%,  $p < 0.005$ ; Monkey P, 35% vs  
534 27%,  $p < 0.05$ , McNemar's test). Post-hoc pairwise testing, however, found no significant differences in  
535 any of the 6 individual cortical areas in either monkey (McNemar's tests with Bonferroni correction for 6  
536 tests,  $p > 0.05/6$ ). Nor did the percent of Connect+ units differ significantly among cortical areas in either  
537 monkey during joystick trials (Monkey Q,  $p > 0.05$ ; Monkey P,  $p > 0.8$ ,  $\chi^2$  tests) or during BCI trials  
538 (Monkey Q,  $p > 0.4$ ; Monkey P,  $p > 0.2$ ,  $\chi^2$  tests). Though not demonstrable for individual cortical areas,  
539 in both monkeys the overall percentage of non-BCI units with effective connectivity to or from BCI units  
540 increased during BCI as compared to joystick control.

541 Non-BCI units providing effective connections to BCI units might play a different role than those receiving  
542 effective connections from BCI units. We therefore classified Connect+ non-BCI units into those with  
543 effective connectivity to a BCI unit (Connect+<sub>trigger</sub>) and those with effective connectivity from a BCI unit  
544 (Connect+<sub>target</sub>). Note that these classes are not mutually exclusive because, although each unit pair can  
545 have only one effective connection, the same non-BCI unit could have an effective connection to one BCI  
546 unit and receive an effective connection from another BCI unit. Percentages of Connect+<sub>trigger</sub> and  
547 Connect+<sub>target</sub> units are given in Table 3, pooling across assignments for each monkey. When pooling across  
548 cortical areas in each animal separately, the percentage of Connect+<sub>trigger</sub> units was not significantly different  
549 from the percentage of Connect+<sub>target</sub> units either during joystick trials or during BCI trials ( $p > 0.05$ ,  
550 McNemar's tests). Nor were significant differences found for any of the individual cortical areas during  
551 either joystick or BCI trials (McNemar's test with Bonferroni correction for 6 tests,  $p > 0.05/6$ ). Thus,  
552 similar percentages of non-BCI units in each cortical area provided effective connections to and received  
553 effective connections from BCI units during each task.

554 As described above, we found that the *nMD* of most BCI units was greater during BCI trials than during  
555 joystick trials, as was the *nMD* of many non-BCI units. Did this increase in *nMD* during BCI trials occur  
556 selectively in Connect+ units as compared to Connect- units? Figure 10 shows a scatterplot for each monkey  
557 in which each point represents the *nMD* for a non-BCI unit during joystick (abscissa) versus BCI (ordinate)  
558 trials, along with the respective marginal probability distributions. Colors distinguish Connect+ (blue)  
559 versus Connect- (orange) units pooled from all assignments in each monkey. More evident in Monkey Q  
560 than in Monkey P is that the majority of Connect+ units lie above the dashed line of unity slope, indicating

561 that on average Connect+ units had a larger *nMD* during BCI trials than during joystick trials, which was  
562 the case in both monkeys (Monkey Q,  $p < 5e-6$ ; Monkey P,  $p < 0.05$ , Wilcoxon signed-rank tests). In  
563 contrast, the population of Connect- neurons showed no systematic joystick versus BCI difference in *nMD*  
564 in either monkey (Monkey Q,  $p > 0.05$ ; Monkey P,  $p > 0.9$ , Wilcoxon signed-rank tests). The marginal  
565 probability distributions confirm this difference between Connect+ and Connect- neurons. During BCI  
566 trials, the median *nMD* of Connect+ units was greater than that of Connect- units in both monkeys (right  
567 histograms, Monkey Q,  $p < 5e-4$ ; Monkey P,  $p < 5e-7$ , Wilcoxon rank-sum tests) whereas during Joystick  
568 trials the median *nMD* of Connect+ and Connect- units was not different (top histograms, Monkey Q,  $p >$   
569  $0.8$ ; Monkey P,  $p > 0.1$ , Wilcoxon rank-sum tests). While the scatterplots of Figure 10 exclude outliers  
570 with *nMD*  $> 1.7$  (6 units from Monkey Q, 9 from Monkey P) for purposes of display, including all outliers  
571 did not change any of these findings. The modulation depth of Connect+ neurons thus increased during  
572 BCI trials while that of Connect- neurons did not.

573

574 **DISCUSSION**

575 The firing rates of neurons in multiple cortical areas are modulated during voluntary upper extremity  
576 movements. We found that while only 4 M1 units controlled a closed-loop BCI, substantial numbers of  
577 non-BCI units not only in frontal motor areas (M1, PMd, PMv) but also in parietal areas (S1, dPPC, AIP)  
578 likewise were modulated in relation to the task. In each of these cortical areas, generally comparable  
579 percentages of non-BCI units were modulated during joystick and BCI control, though in Monkey Q the  
580 percentage was significantly higher during BCI trials in M1, PMd, and AIP. Many non-BCI units were  
581 cosine-tuned during both joystick- and BCI-control of the cursor, and among these units we found changes  
582 in preferred direction, modulation depth, and effective connectivity during BCI trials as compared to  
583 joystick trials, similar to the changes that occurred concurrently in the BCI units. All these cortical areas  
584 thus participate, not only in natural control of voluntary limb movement, but in a more general system for  
585 closed-loop control of an effector being moved to a visual target. And many individual non-BCI neurons  
586 in these areas change their activity between joystick and BCI control.

587 Our findings have two important limitations. First, whereas the joystick-controlled movements typically  
588 had a large rapid and relatively ballistic initial component that often brought the cursor promptly to the  
589 target, the BCI-controlled movements were generally slower and less smooth, often requiring multiple  
590 corrective sub-movements before arriving in the target (Figure 4). This difference was particularly evident  
591 because we chose to use a more permissive center-out task for BCI-controlled trials and chose not to train  
592 the monkeys to the point of BCI performance equivalent to that with joystick control. Some of our findings  
593 may have resulted from these differences between the present joystick- versus BCI-controlled trials. The  
594 latter might be viewed as a comparatively early stage in learning to use a difficult, non-intuitive controller.

595 Second, rather than focusing our recording channel capacity on one or two cortical areas, for the present  
596 study we distributed the available channels across six cortical areas. Fewer units therefore were recorded  
597 from any one area than in some other studies. Furthermore, across BCI-assignments in a given monkey  
598 and across monkeys, our microelectrode arrays consistently recorded fewer analyzable units in parietal than  
599 in frontal cortical areas (Table 1). The number of units recorded may have limited the present statistical  
600 comparisons among areas. Had we recorded more units, particularly in S1, dPPC, and AIP, additional  
601 significant differences might have emerged. Nevertheless, we have included these parietal areas along with  
602 the frontal areas in the present analyses as providing our best available sampling of their activity.

603 *Strategies and cognitive load elicited by the BCI decoder*

604 For the present study, we intentionally chose a non-intuitive BCI decoder to require a relatively high  
605 cognitive load, potentially eliciting more extensive activity in the various cortical areas from which we  
606 recorded. Because using fewer units tends to make BCI control less accurate (Law et al., 2014), we limited  
607 the number of BCI units to four, and assigned each BCI unit arbitrarily to drive cursor velocity in a particular  
608 cardinal direction without regard to its preferred direction during joystick trials. Under such conditions  
609 BCI control can be achieved through a variety of strategies, including remapping the preferred directions  
610 of individual BCI units, reweighting their modulation depths, and re-aiming with a coherent rotation of the  
611 preferred directions of most units (Jarosiewicz et al., 2008; Ganguly et al., 2011; Chase et al., 2012;  
612 Sakellari et al., 2019). Across the eight assignments in the two monkeys, preferred directions changed

613 significantly in all but one of the BCI units that were also modulated during the joystick task. On average  
614 the PD of each BCI unit shifted toward its own assigned direction, with some changing in clockwise and  
615 others in counterclockwise directions in five of the eight assignments. In addition, the average modulation  
616 depth of the BCI units increased in every assignment. In only one of the eight assignments did the  
617 population of non-BCI units show evidence of a coherent rotation all in the same direction. Whereas  
618 remapping and reweighting thus occurred in most assignments, re-aiming was uncommon.

619 Our BCI decoder design was sufficiently difficult for the monkeys to use that we relaxed our criteria for  
620 successful trial performance compared to joystick trials. Even after several days of BCI training when the  
621 monkeys had achieved our criteria of > 80% success over at least 400 trials, cursor trajectories remained  
622 considerably longer and more convoluted during BCI trials than during joystick trials, and non-BCI units  
623 remained as deeply modulated during BCI trials as during joystick trials (Hwang et al., 2013; Law et al.,  
624 2014). Had we used a BCI decoder optimized to incorporate the natural tuning of larger numbers of M1  
625 neurons (Jarosiewicz et al., 2008; Ganguly and Carmena, 2009; Gilja et al., 2012; Sadtler et al., 2014)  
626 and/or trained the monkeys for substantially more sessions (Oby et al., 2019; Zhou et al., 2019), the response  
627 time and path length of BCI trials might have more closely approximated that of joystick trials, and the  
628 modulation of non-BCI units might have diminished (Ganguly et al., 2011; Clancy et al., 2014). The present  
629 results most likely were obtained, therefore, while the monkeys still employed some degree of cognitive  
630 exploration that had not yet consolidated to automatic execution (Wander et al., 2013).

631 In controlling natural movements of the upper extremity, patterns of co-activation in M1 neurons are largely  
632 confined to an “intrinsic manifold” in the neural state-space (Sadtler et al., 2014; Gallego et al., 2018;  
633 Gallego et al., 2020). Learning to control a BCI with M1 neurons progresses more quickly if the BCI  
634 decoder uses latent dimensions within this intrinsic manifold than if patterns outside the manifold are  
635 required (Sadtler et al., 2014). When such out-of-manifold patterns are required by the decoder, novel  
636 patterns of neural co-activation must be learned over many sessions (Oby et al., 2019). The time needed  
637 by the present monkeys to achieve our proficiency criteria for BCI performance, together with changes in  
638 the preferred directions and modulation depths of the BCI units, suggests that our BCI decoder most often  
639 constituted an out-of-manifold perturbation that required learning new patterns of unit co-activation. The  
640 newly learned patterns were not necessarily confined to the BCI units, and may have involved many non-  
641 BCI units in various cortical areas as well.

#### 642 *Variability of changes observed*

643 Although the present BCI units consistently showed changes in preferred direction and modulation depth  
644 in all assignments, the concurrent changes observed in non-BCI units were comparatively variable across  
645 assignments, both within and between monkeys. Such variability might suggest that the activity of non-  
646 BCI units in some or all cortical areas was an epiphenomenon, irrelevant or even counter-productive to  
647 closed loop BCI performance. We consider this possibility to be unlikely, however. Although we cannot  
648 determine the exact causes of this variability, we suggest two potential factors that may have contributed.

649 First, as indicated by their success rates, response times, and cursor path lengths, the two monkeys  
650 approached the joystick and BCI tasks differently, with Monkey P performing better at the joystick task  
651 while Monkey Q achieved better performance at the BCI task. Our two subjects thus may have been at

652 different positions on the spectrum from BCI learners to non-learners (Bridges et al., 2020). The behavioral  
653 differences between the two monkeys were accompanied by differences in neural activity. Non-BCI units  
654 in Monkey Q showed more consistent increases in the percent of units modulated, their modulation depths,  
655 and their effective connectivity with other units during BCI as compared to joystick trials than did non-BCI  
656 units in Monkey P. We speculate that the differences between the two monkeys in behavioral performance  
657 and in neural activity were interrelated, and were related as well to a difference in what appeared to be the  
658 monkey's engagement in performing the BCI task.

659 Second, within a given animal, each different BCI-unit assignment likely required a different pattern of  
660 coactivation among the BCI units (Athalye et al., 2017; Oby et al., 2019). These different coactivation  
661 patterns among the BCI units may have been achieved with different patterns of activity in non-BCI units  
662 in the various cortical areas examined here, producing varying results from assignment to assignment within  
663 each subject. Although the BCI units were solely responsible for directly controlling the BCI output, a  
664 closed-loop BCI cannot be operated successfully without engaging the activity of at least some non-BCI  
665 units. The BCI units in our task must at least have received processed visual information about the location  
666 of the peripheral target and likely received visual feedback about the current location of the cursor. This  
667 information could only have come through non-BCI units, though not necessarily those that we recorded.  
668 In addition, internal decisions about when to initiate another trial probably influenced the BCI units, and  
669 their firing may also have provided efference copy to circuits comparing a forward model of the expected  
670 cursor trajectory with the actual incoming feedback. We speculate that, released from the need to control  
671 the motion of the cursor with movement of the native upper extremity, and with an expansive neural space  
672 available, the CNS found ways to provide these functions that varied to some extent from assignment to  
673 assignment.

#### 674 *Effective connectivity of non-BCI units and BCI control*

675 A previous study has shown that effective connectivity among the M1 BCI units controlling a reach-to-  
676 grasp robot changes progressively as non-human primates acquired proficient control, though the time  
677 course of these changes differed depending on whether the M1 BCI population was contralateral or  
678 ipsilateral to an upper extremity amputation (Balasubramanian et al., 2017). Here, we found that effective  
679 connectivity increased during BCI as compared to joystick control in one monkey but not the other. But in  
680 both monkeys, non-BCI units with effective connectivity to or from a BCI unit (Connect+ units) on average  
681 had higher normalized modulation depths during BCI trials than those without such connectivity (Connect-  
682 units). Our simulation (see Methods) indicates that this difference cannot be attributed simply to a higher  
683 likelihood of finding false positive connections for units with larger modulation depth. We therefore  
684 speculate that Connect+ non-BCI units are more likely than Connect- units to have played a relatively direct  
685 role in one or more of the ancillary functions required for closed-loop control—processing target location,  
686 inverse model, visual feedback, efference copy, forward model, etc. Although current concepts of cortico-  
687 cortical information flow during voluntary movement emphasize transmission of information from  
688 posterior parietal cortex to premotor cortex and then to primary motor cortex (Rizzolatti et al., 1998;  
689 Grafton, 2010), we found that effective connectivity between BCI and non-BCI units in most of the cortical  
690 areas we examined was largely bidirectional, both during joystick and during BCI trials. Our estimates of  
691 effective connectivity of course are based on statistical models and do not represent actual synaptic  
692 connectivity. But with the exception of dPPC, where we found no effective connectivity with BCI units

693 during BCI trials, we found that similar fractions of non-BCI units in all cortical areas had effective  
694 connectivity to and effective connectivity from the BCI units in M1.

695 *Conclusions*

696 The present study shows for the first time that changes in preferred direction, modulation depth, and  
697 effective connectivity occur in units beyond the cortical area(s) that directly control a BCI and extend to  
698 many, though not all, cortical areas involved in the distributed cortical network for the sensorimotor control  
699 of voluntary movements. In theory, given that the performance of modern neuroprostheses falls short of  
700 natural control of a native limb (Hochberg et al., 2012; Rouse and Schieber, 2015; Wodlinger et al., 2015),  
701 harnessing the activity of units from multiple cortical areas in next generation BCIs might provide a more  
702 dexterous neuroprosthetic extremity. Further studies, ideally recording more units in each area, will be  
703 needed to extend the present findings to the more proficient performance achieved with BCI decoders  
704 optimized to incorporate the natural tuning of large numbers of neurons, and to determine whether non-BCI  
705 units play similar or different functional roles in closed-loop control of the native limb versus a BCI.

706

707 **REFERENCES**

- 708 Andersen RA, Aflalo T, Kellis S (2019) From thought to action: The brain-machine interface in posterior  
709 parietal cortex. *Proc Natl Acad Sci U S A*.
- 710 Arduin PJ, Fregnac Y, Shulz DE, Ego-Stengel V (2014) Bidirectional control of a one-dimensional robotic  
711 actuator by operant conditioning of a single unit in rat motor cortex. *Front Neurosci* 8:206.
- 712 Ashe J, Georgopoulos AP (1994) Movement parameters and neural activity in motor cortex and area 5.  
713 *Cerebral Cortex* 4:590-600.
- 714 Athalye VR, Ganguly K, Costa RM, Carmena JM (2017) Emergence of Coordinated Neural Dynamics  
715 Underlies Neuroprosthetic Learning and Skillful Control. *Neuron* 93:955-970 e955.
- 716 Bakola S, Passarelli L, Huynh T, Impieri D, Worthy KH, Fattori P, Galletti C, Burman KJ, Rosa MGP  
717 (2017) Cortical Afferents and Myeloarchitecture Distinguish the Medial Intraparietal Area (MIP)  
718 from Neighboring Subdivisions of the Macaque Cortex. *eNeuro* 4.
- 719 Balasubramanian K, Vaidya M, Southerland J, Badreldin I, Eleryan A, Takahashi K, Qian K, Slutzky MW,  
720 Fagg AH, Oweiss K, Hatsopoulos NG (2017) Changes in cortical network connectivity with long-  
721 term brain-machine interface exposure after chronic amputation. *Nat Commun* 8:1796.
- 722 Batista AP, Andersen RA (2001) The parietal reach region codes the next planned movement in a sequential  
723 reach task. *J Neurophysiol* 85:539-544.
- 724 Berens P (2009) CircStat: A MATLAB Toolbox for Circular Statistics. *J Stat Softw* 31:1-21.
- 725 Bridges N, Stickle M, Moxon K (2020) Transitioning from global to local computational strategies during  
726 brain-machine interface learning. *bioRxiv*:3-8.
- 727 Chase SM, Kass RE, Schwartz AB (2012) Behavioral and neural correlates of visuomotor adaptation  
728 observed through a brain-computer interface in primary motor cortex. *J Neurophysiol* 108:624-644.
- 729 Chestek CA, Batista AP, Santhanam G, Yu BM, Afshar A, Cunningham JP, Gilja V, Ryu SI, Churchland  
730 MM, Shenoy KV (2007) Single-neuron stability during repeated reaching in macaque premotor  
731 cortex. *Journal of Neuroscience* 27:10742-10750.
- 732 Clancy KB, Koralek AC, Costa RM, Feldman DE, Carmena JM (2014) Volitional modulation of optically  
733 recorded calcium signals during neuroprosthetic learning. *Nat Neurosci* 17:807-809.
- 734 De Vitis M, Breveglieri R, Hadjimitsakis K, Vanduffel W, Galletti C, Fattori P (2019) The neglected  
735 medial part of macaque area PE: segregated processing of reach depth and direction. *Brain Struct*  
736 *Funct* 224:2537-2557.
- 737 Downey JE, Schwed N, Chase SM, Schwartz AB, Collinger JL (2018) Intracortical recording stability in  
738 human brain-computer interface users. *J Neural Eng* 15:046016.
- 739 Fetz EE (1969) Operant conditioning of cortical unit activity. *Science* 163:955-958.
- 740 Fraser GW, Schwartz AB (2012) Recording from the same neurons chronically in motor cortex. *J*  
741 *Neurophysiol* 107:1970-1978.

- 742 Gallego JA, Perich MG, Chowdhury RH, Solla SA, Miller LE (2020) Long-term stability of cortical  
743 population dynamics underlying consistent behavior. *Nat Neurosci* 23:260-270.
- 744 Gallego JA, Perich MG, Naufel SN, Ethier C, Solla SA, Miller LE (2018) Cortical population activity  
745 within a preserved neural manifold underlies multiple motor behaviors. *Nature Communications* In  
746 Press:1-13.
- 747 Ganguly K, Dimitrov DF, Wallis JD, Carmena JM (2011) Reversible large-scale modification of cortical  
748 networks during neuroprosthetic control. *Nat Neurosci* 14:662-667.
- 749 Georgopoulos AP, Kalaska JF, Caminiti R, Massey JT (1982) On the relations between the direction of  
750 two-dimensional arm movements and cell discharge in primate motor cortex. *Journal of*  
751 *Neuroscience* 2:1527-1537.
- 752 Golub MD, Sadtler PT, Oby ER, Quick KM, Ryu SI, Tyler-Kabara EC, Batista AP, Chase SM, Yu BM  
753 (2018) Learning by neural reassociation. *Nat Neurosci* 21:607-616.
- 754 Grafton ST (2010) The cognitive neuroscience of prehension: recent developments. *Exp Brain Res*  
755 204:475-491.
- 756 Hochberg LR, Bacher D, Jarosiewicz B, Masse NY, Simeral JD, Vogel J, Haddadin S, Liu J, Cash SS, van  
757 der Smagt P, Donoghue JP (2012) Reach and grasp by people with tetraplegia using a neurally  
758 controlled robotic arm. *Nature* 485:372-375.
- 759 Hwang EJ, Bailey PM, Andersen RA (2013) Volitional control of neural activity relies on the natural motor  
760 repertoire. *Curr Biol* 23:353-361.
- 761 Jarosiewicz B, Chase SM, Fraser GW, Velliste M, Kass RE, Schwartz AB (2008) Functional network  
762 reorganization during learning in a brain-computer interface paradigm. *ProcNatlAcadSciUSA*  
763 105:19486-19491.
- 764 Kalaska JF, Caminiti R, Georgopoulos AP (1983) Cortical mechanisms related to the direction of two-  
765 dimensional arm movements: relations in parietal area 5 and comparison with motor cortex.  
766 *Experimental Brain Research* 51:247-260.
- 767 Kihlberg JK, Herson JH, Schotz WE (1972) Square Root Transformation Revisited. *J Roy Stat Soc C-App*  
768 21:76-&.
- 769 Kim S, Putrino D, Ghosh S, Brown EN (2011) A Granger causality measure for point process models of  
770 ensemble neural spiking activity. *PLoS Comput Biol* 7:e1001110.
- 771 Koch C (2004) *Biophysics of Computation : Information Processing in Single Neurons*. ProQuest Ebook  
772 Central: Oxford University Press.
- 773 Koralek AC, Jin X, Long JD, 2nd, Costa RM, Carmena JM (2012) Corticostriatal plasticity is necessary for  
774 learning intentional neuroprosthetic skills. *Nature* 483:331-335.
- 775 Law AJ, Rivlis G, Schieber MH (2014) Rapid acquisition of novel interface control by small ensembles of  
776 arbitrarily selected primary motor cortex neurons. *J Neurophysiol* 112:1528-1548.

- 777 Lebedev MA, Nicolelis MA (2017) Brain-Machine Interfaces: From Basic Science to Neuroprostheses and  
778 Neurorehabilitation. *Physiol Rev* 97:767-837.
- 779 Mollazadeh M, Aggarwal V, Davidson AG, Law AJ, Thakor NV, Schieber MH (2011) Spatiotemporal  
780 variation of multiple neurophysiological signals in the primary motor cortex during dexterous  
781 reach-to-grasp movements. *J Neurosci* 31:15531-15543.
- 782 Moran DW, Schwartz AB (1999) Motor cortical representation of speed and direction during reaching.  
783 *Journal of Neurophysiology* 82:2676-2692.
- 784 Moritz CT, Perlmutter SI, Fetz EE (2008) Direct control of paralysed muscles by cortical neurons. *Nature*  
785 456:639-642.
- 786 Moxon KA, Foffani G (2015) Brain-machine interfaces beyond neuroprosthetics. *Neuron* 86:55-67.
- 787 Nazarpour K, Barnard A, Jackson A (2012) Flexible cortical control of task-specific muscle synergies. *J*  
788 *Neurosci* 32:12349-12360.
- 789 Oby ER, Golub MD, Hennig JA, Degenhart AD, Tyler-Kabara EC, Yu BM, Chase SM, Batista AP (2019)  
790 New neural activity patterns emerge with long-term learning. *Proc Natl Acad Sci U S A* 116:15210-  
791 15215.
- 792 Prud'homme MJ, Cohen DA, Kalaska JF (1994) Tactile activity in primate primary somatosensory cortex  
793 during active arm movements: cytoarchitectonic distribution. *Journal of Neurophysiology* 71:173-  
794 181.
- 795 Rajalingham R, Musallam S (2017) Characterization of neurons in the primate medial intraparietal area  
796 reveals a joint representation of intended reach direction and amplitude. *PLoS One* 12:e0182519.
- 797 Rizzolatti G, Luppino G, Matelli M (1998) The organization of the cortical motor system: new concepts.  
798 *Electroencephalography and Clinical Neurophysiology* 106:283-296.
- 799 Rouse AG, Schieber MH (2015) Advancing brain-machine interfaces: moving beyond linear state space  
800 models. *Front Syst Neurosci* 9:108.
- 801 Rouse AG, Schieber MH (2016) Spatiotemporal Distribution of Location and Object Effects in Primary  
802 Motor Cortex Neurons during Reach-to-Grasp. *J Neurosci* 36:10640-10653.
- 803 Sadtler PT, Quick KM, Golub MD, Chase SM, Ryu SI, Tyler-Kabara EC, Yu BM, Batista AP (2014) Neural  
804 constraints on learning. *Nature* 512:423-426.
- 805 Sakellaridi S, Christopoulos VN, Aflalo T, Pejsa KW, Rosario ER, Ouellette D, Pouratian N, Andersen RA  
806 (2019) Intrinsic Variable Learning for Brain-Machine Interface Control by Human Anterior  
807 Intraparietal Cortex. *Neuron* 102:694-705 e693.
- 808 Shadmehr R, Krakauer JW (2008) A computational neuroanatomy for motor control. *Exp Brain Res*  
809 185:359-381.
- 810 Stark E, Asher I, Abeles M (2007) Encoding of reach and grasp by single neurons in premotor cortex is  
811 independent of recording site. *J Neurophysiol* 97:3351-3364.

- 812 Wander JD, Blakely T, Miller KJ, Weaver KE, Johnson LA, Olson JD, Fetz EE, Rao RP, Ojemann JG  
813 (2013) Distributed cortical adaptation during learning of a brain-computer interface task. *Proc Natl*  
814 *Acad Sci U S A* 110:10818-10823.
- 815 Wodlinger B, Downey JE, Tyler-Kabara EC, Schwartz AB, Boninger ML, Collinger JL (2015) Ten-  
816 dimensional anthropomorphic arm control in a human brain-machine interface: difficulties,  
817 solutions, and limitations. *J Neural Eng* 12:016011.
- 818 Zhou X, Tien RN, Ravikumar S, Chase SM (2019) Distinct types of neural reorganization during long-term  
819 learning. *J Neurophysiol* 121:1329-1341.
- 820

821 **FIGURE LEGENDS**

822 Figure 1. Center-out task. The monkey controlled the movement of the cursor (white “+”) from the center  
823 to the peripheral target.

824 Figure 2. Location of arrays. **A)** Monkey Q. **B)** Monkey P. Array locations and cortical sulci were  
825 redrawn from intraoperative photographs. CS, Central Sulcus; AS, Arcuate Sulcus; SPS, Superior  
826 Precentral Sulcus. IPS, Intraparietal Sulcus. Orientation arrows: M, Medial; C, Caudal.

827 Figure 3. BCI training. Success rates (**A**) and mean response times (**B**) are shown in sequential blocks of  
828 50 successfully performed trials over 10 daily training sessions. As success rates increased,  
829 response times (from the appearance of the Go cue until the cursor had been in the target for 50  
830 ms) decreased. The number of blocks of 50 successful trials varied from one training day to the  
831 next. Data from Monkey Q, assignment ii.

832 Figure 4. Cursor paths in joystick trials (**A**) and BCI trials (**B**). Each trial started within the center target  
833 (blue circle) and ended in one of the eight peripheral targets (between the red and yellow circles).  
834 Thin lines show the cursor paths to each target (colors blue to brown) from 5 successful trials, and  
835 thick lines represent cursor paths averaged across 20 successful trials to each target (time  
836 normalized between *Go Cue* and *Success* events). Squares and solid dots show the cursor  
837 positions at the time of *Go Cue* and *Success*, respectively. Data from Monkey Q, assignment iii.

838 Figure 5. Percent of units modulated significantly with the center-out task during joystick trials and  
839 during BCI trials. **A.** Monkey Q. **B.** Monkey P. Bars represent the percentages of units across all  
840 assignments during joystick trials (white) or BCI trials (grey), while colored lines compare  
841 percentages during joystick trials (open circles) vs. BCI trials (filled circles) in individual BCI  
842 assignments. Because all BCI M1 units were modulated during the BCI task, closed circles  
843 overlap for those units at 100%. Open circles and colored lines also overlapped at 100% for BCI  
844 units during joystick trials for Monkey Q in assignments i and ii.

845 Figure 6. Preferred direction changes in a single session. Lines indicate the  $\Delta PD$  of the 4 BCI units (blue),  
846 29 non-BCI units (red) in polar coordinates. The yellow histogram represents the bootstrapped  
847 probability distribution of  $\Delta PD$ s under the null hypothesis of no change. All four BCI units, as  
848 well as 72% of the non-BCI units, had a significant preferred direction change during BCI trials  
849 compared to joystick trials. At the population level, the  $\Delta PD$  among non-BCI units was not  
850 significantly different from  $0^\circ$ . Data from Monkey Q, BCI assignment ii.

851 Figure 7. Normalized Modulation Depth (*nMD*) of significantly modulated units during joystick trials  
852 versus BCI trials. **A.** Monkey Q. **B.** Monkey P. Bars represent the median *nMD* among units  
853 across all assignments during joystick trials (white) or BCI trials (grey), while colored lines  
854 compare median *nMD*s during joystick trials (open circles) vs. BCI trials (filled circles) in  
855 individual BCI assignments.

856 Figure 8. Granger connectivity matrices in a single session. Granger connectivity was evaluated  
857 separately during joystick trials (**A**) and during BCI trials (**B**). Each red or blue cell indicates  
858 significant excitatory or inhibitory connectivity from a trigger unit (abscissa) to a target unit  
859 (ordinate). White cells indicate no significant connectivity between the pair. Black lines separate

860 groups of BCI units and non-BCI units from different cortical areas. Data from Monkey Q,  
861 assignment iii.

862 Figure 9. The fraction of unit pairs with significant effective connectivity during joystick-controlled trials  
863 (white bars) and BCI-controlled trials (grey bars) for Monkey Q (**A**) and Monkey P (**B**). For each  
864 monkey, overall fractions are shown to the left and the fractions with excitatory or inhibitory  
865 connectivity are shown separately to the right. White and grey bars represent fractions pooled for  
866 each monkey across assignments (with p-values from McNemar's tests), while colored lines  
867 represent the individual BCI-unit assignments.

868 Figure 10. Normalized modulation depths (*nMD*) of Connect+ units and Connect- units compared during  
869 joystick versus BCI trials. (**A**) Monkey Q. (**B**) Monkey P. Scatter plots show that the *nMDs* of  
870 Connect+ units (blue circles) were higher during BCI trials, as the majority of blue circles fall  
871 above the dashed line of unity slope. The same was not true for Connect- units (orange circles).  
872 Marginal histograms show the probability distributions of Connect+ *nMDs* (blue) and Connect-  
873 *nMDs* (orange) during BCI trials (right) which were significantly different, and during joystick  
874 trials (top) which were not. Blue and orange arrows represent the medians for Connect+ and  
875 Connect- unit populations, respectively. In these scatterplots, outliers with *nMD* > 1.7 have been  
876 excluded for purposes of display; including the outliers did not change the results.

877

878 TABLES

879 Table 1. Number of units analyzed for each BCI assignment. The three values in each cell give the number of: unique  
 880 units | units modulated significantly during joystick and/or BCI trials | units modulated significantly during  
 881 both joystick and BCI trials.

	Monkey Q						Monkey P			
	i	ii	iii	iv	v	total	i	ii	iii	total
<b>BCI units</b>	4 4 4	4 4 4	4 4 2	4 4 3	4 4 4	20 20 17	4 4 3	4 4 4	4 4 2	12 12 9
<b>Non-BCI</b>										
<b>M1</b>	38 30 11	30 26 14	34 30 15	23 20 10	35 35 25	160 141 75	102 87 61	125 89 32	104 73 29	331 249 122
<b>PMd</b>	9 6 4	21 18 7	12 10 2	8 7 5	16 15 8	66 56 26	28 25 18	23 17 11	30 27 16	81 69 45
<b>PMv</b>	23 16 3	16 12 3	10 8 4	17 10 9	20 18 10	86 64 29	23 11 6	24 11 3	14 9 1	61 31 10
<b>S1</b>	7 4 4	4 2 0	7 3 1	5 2 0	5 4 2	28 15 7	14 13 8	22 16 6	18 8 1	54 37 15
<b>dPPC</b>	5 0 0	9 5 3	3 2 1	11 7 0	10 6 2	38 20 6	15 12 6	6 3 1	13 3 2	34 18 9
<b>AIP</b>	8 5 3	7 4 2	5 4 2	5 4 3	5 5 2	30 22 12	8 6 2	16 9 2	14 10 2	38 25 6

882

883 Table 2. Percent of units with a significant joystick vs. BCI change in preferred direction

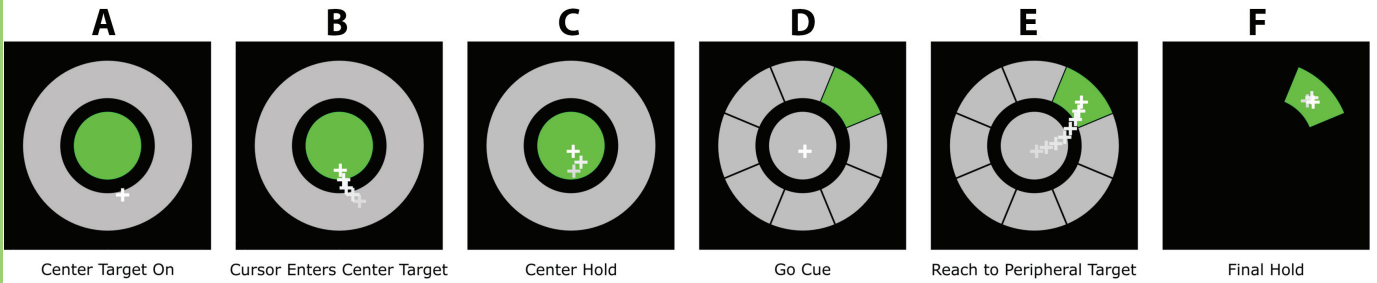
	<b>BCI units</b>	<b>Non-BCI:</b>	<b>M1</b>	<b>PMd</b>	<b>PMv</b>	<b>S1</b>	<b>dPPC</b>	<b>AIP</b>	<b>All</b>
<b>Monkey Q</b>	100%		84%	81%	52%	86%	33%	42%	72%
<b>Monkey P</b>	89%		77%	67%	60%	87%	78%	67%	74%

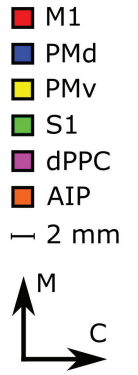
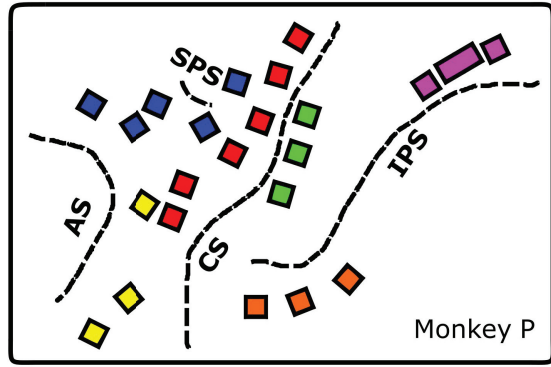
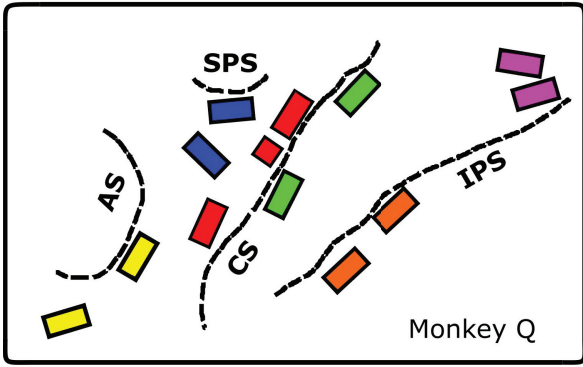
884

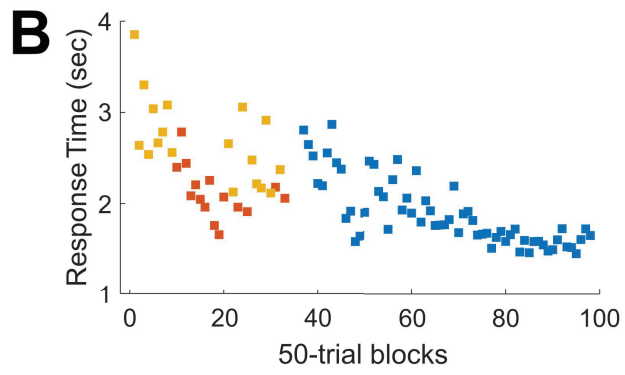
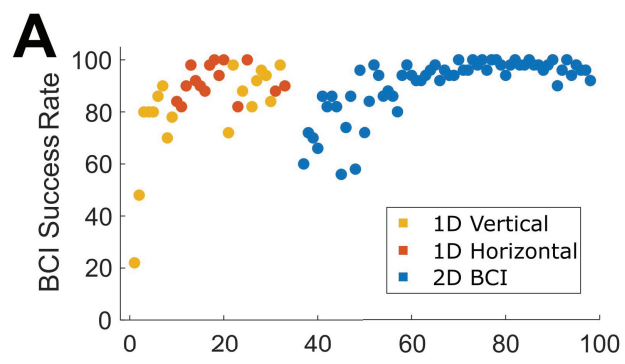
885 Table 3. Percentages of Connect+ non-BCI units

Monkey	Task	<i>Non-BCI units:</i>	M1	PMd	PMv	S1	dPPC	AIP	Overall
Monkey Q	Joystick	Connect+	27	12	14	57	17	8	21
		Connect+ <sub>trigger</sub>	20	4	4	14	0	8	13
		Connect+ <sub>target</sub>	13	8	10	43	17	8	13
	BCI	Connect+	36	42	38	43	0	25	36
		Connect+ <sub>trigger</sub>	23	27	21	14	0	17	21
		Connect+ <sub>target</sub>	32	35	21	43	0	8	28
Monkey P	Joystick	Connect+	30	20	30	27	22	17	27
		Connect+ <sub>trigger</sub>	18	11	20	13	0	17	15
		Connect+ <sub>target</sub>	19	11	20	20	22	0	17
	BCI	Connect+	38	36	20	40	0	33	35
		Connect+ <sub>trigger</sub>	23	20	10	7	0	33	20
		Connect+ <sub>target</sub>	25	20	10	33	0	0	22

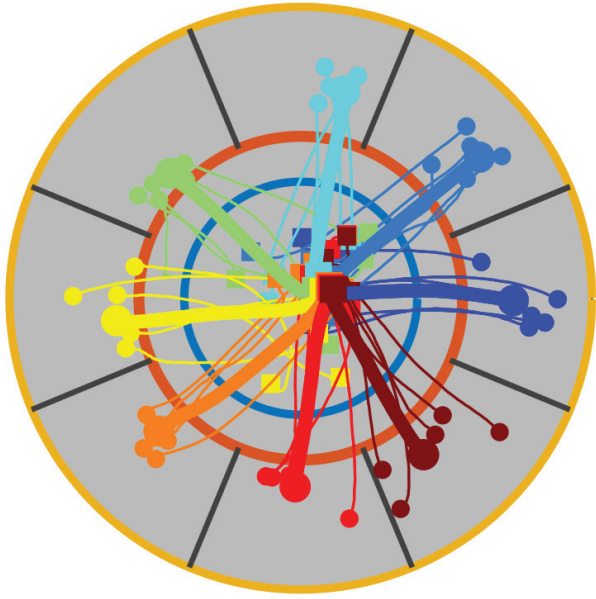
886



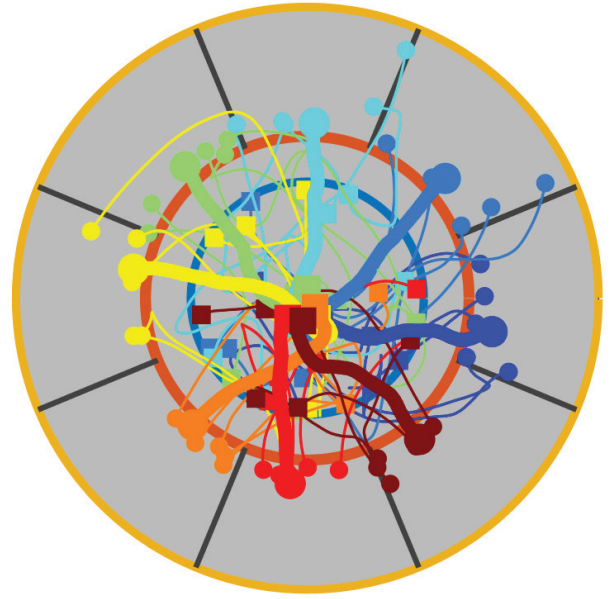


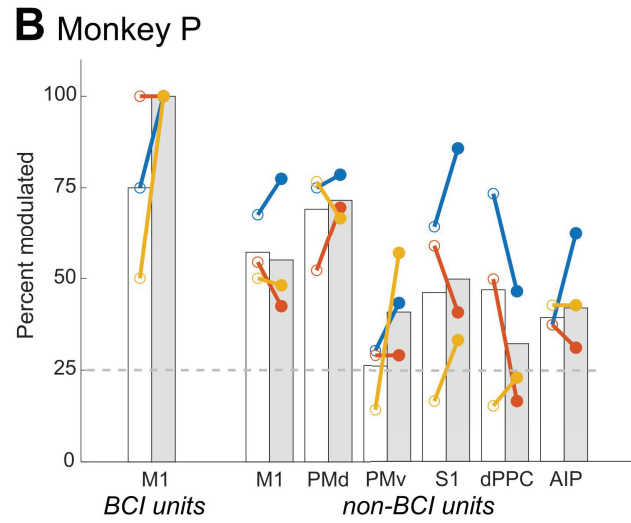
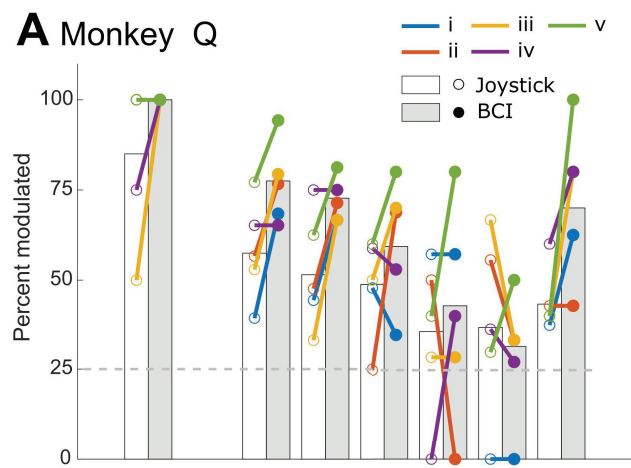


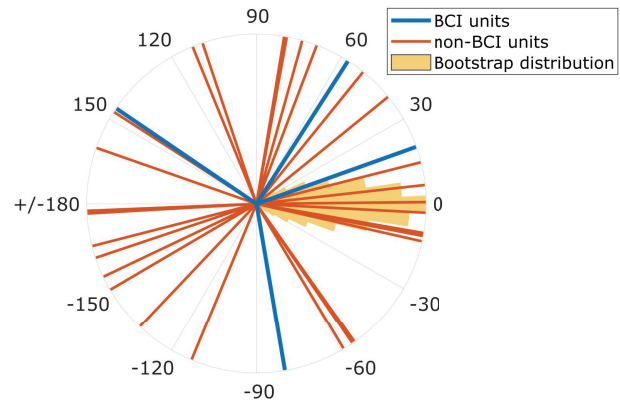
**A** Joystick

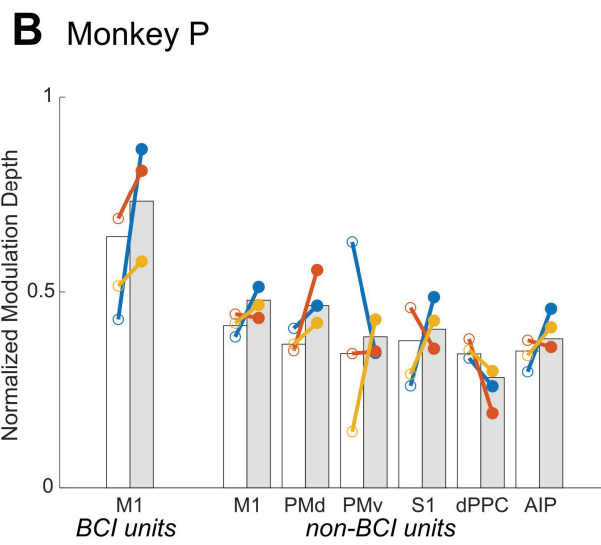
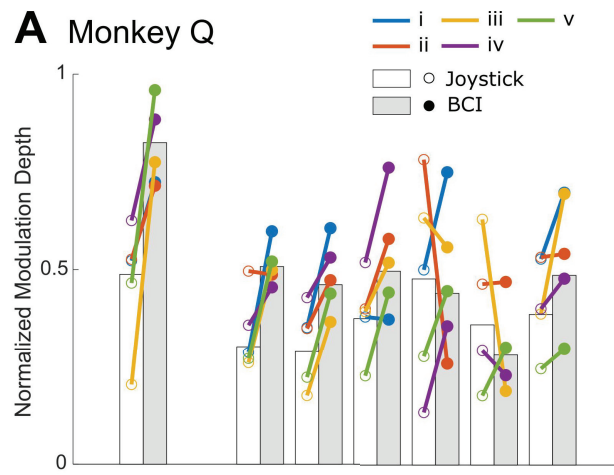


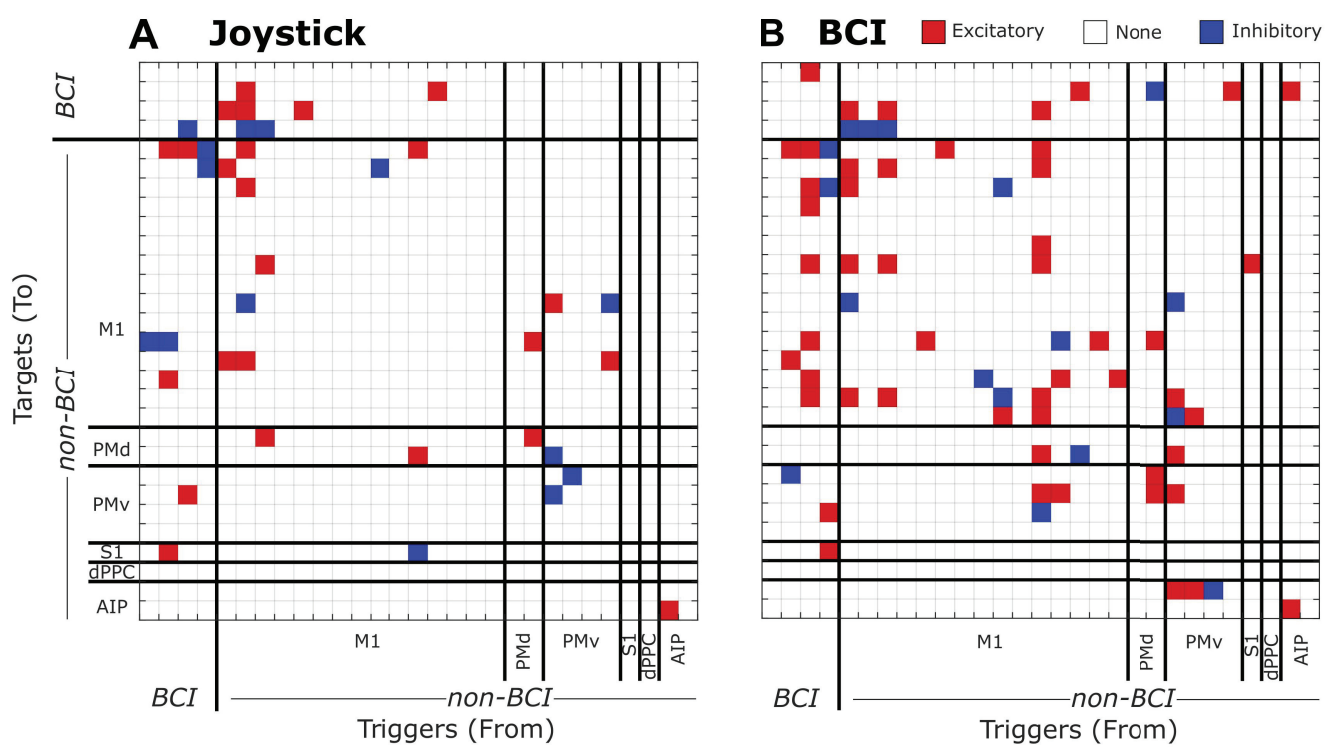
**B** BCI

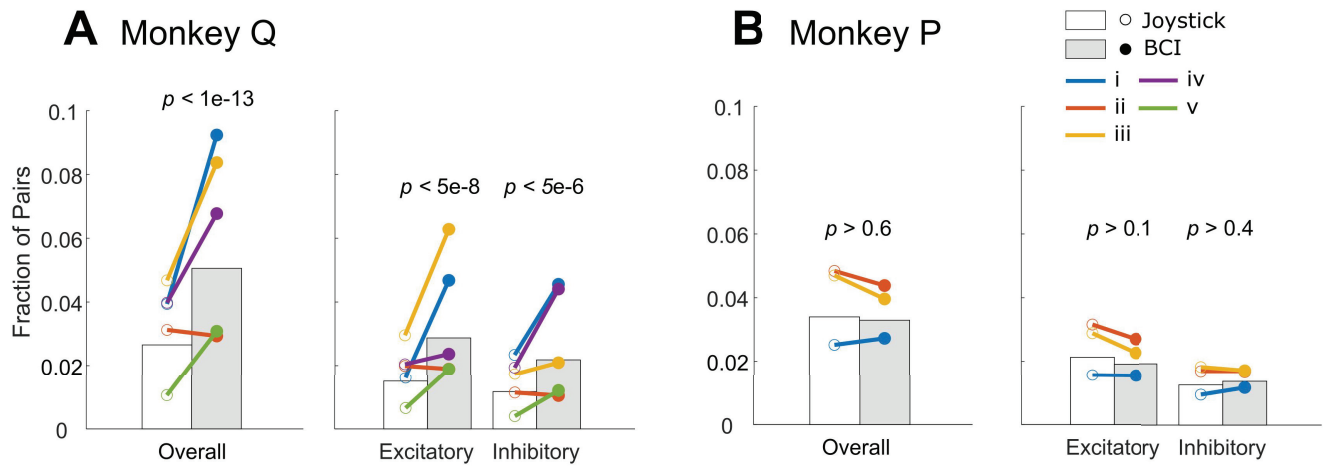




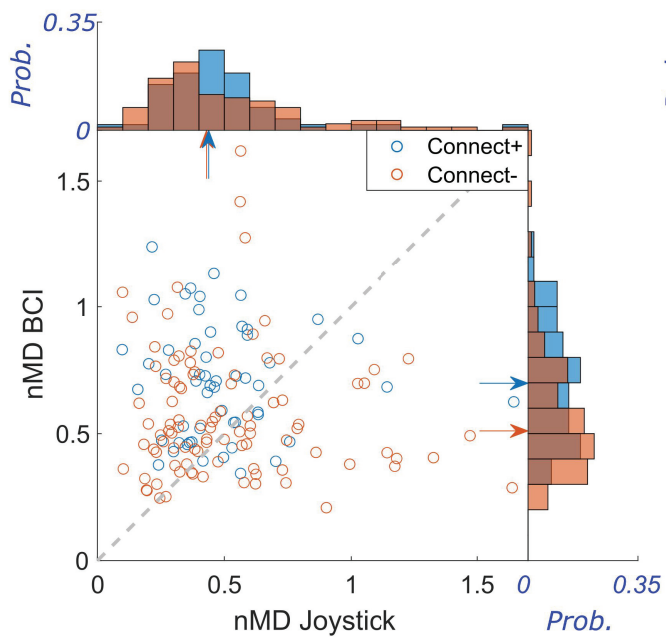








**A** Monkey Q



**B** Monkey P

